J Porous Mater (2017) 24:721–729
DOI 10.1007/s10934-016-0309-6

Proton conductivity and morphology of new composite membranes based on zirconium phosphates, phosphotungstic acid, and silicic acid for direct hydrocarbon fuel cells applications

Amani Al-Othman[1,3] · Yuanchen Zhu[2,3] · Muhammad Tawalbeh[4] · André Y. Tremblay[2] · Marten Ternan[2,3,5]

Published online: 2 November 2016

Abstract The effect of Phosphotungstic acid (PWA) on the proton conductivity and morphology of zirconium phosphate (ZrP), porous polytetrafluoethylene (PTFE), glycerol (GLY) composite membrane was investigated in this work. The composite membranes were synthesized using two approaches: (1) Phosphotungstic acid (PWA) added to phosphoric acid and, (2) PWA + silicic acid were added to phosphoric acid. ZrP was formed inside the pores of PTFE via the in situ precipitation. The membranes were evaluated for their morphology and proton conductivity. The proton conductivity of PWA–ZrP/PTFE/GLY membrane was 0.003 S cm^{-1}. When PWA was combined with silicic acid, the proton conductivity increased from 0.003 to 0.059 S cm^{-1} (became about 60% of Nafion's). This conductivity is higher than the proton conductivity of Nafion–silica–PWA membranes reported in the literature. The SEM results showed a porous structure for the modified membranes. The porous structure combined with this reasonable proton conductivity would make these membranes suitable as the electrolyte component in the catalyst layer for direct hydrocarbon fuel cell applications.

Keywords Zirconium phosphate · Phosphotungstic-silicic acid membranes · Proton conductivity · Hydrocarbon fuel cells

1 Introduction

Most proton exchange membrane (PEM) fuel cells currently operate using hydrogen or methanol as fuels. Hydrocarbons are desirable fuels for PEM fuel cells for several reasons including: ease of transportation, availability, and well established infra structure. The use of hydrocarbon fuel cells is proposed to meet modest electricity needs in rural areas. The capital cost of a PEM fuel cell system can be lowered if hydrocarbon fuels are directly fed into the fuel cell anode. This is the result of the elimination of the fuel processor unit required to produce hydrogen or methanol. Despite their several advantages, hydrocarbon fuels still suffer from one major drawback which is their small reaction rates [1]. Hence, high temperature operation is favored.

The performance of direct hydrocarbon fuel cells was recently addressed. A two dimensional CFD model for a high temperature, direct propane fuel cell anode was developed by Khakdaman et al. [2]. The results showed an improvement of the anodic performance at high temperatures. One-third less resistance was obtained at 150 °C using zirconium phosphate (ZrP) as an electrolyte and platinum as a catalyst. Khakdaman et al. [3] developed a two–dimensional CFD model that describes the performance of a complete direct propane fuel cell with a ZrP–PTFE composite membrane, at 150 °C. Modelling results

✉ Amani Al-Othman
aalothman@aus.edu

[1] Department of Chemical Engineering, American University of Sharjah, PO Box 26666, Sharjah, UAE

[2] Chemical and Biological Engineering, University of Ottawa, 161 Louis Pasteur, Ottawa, ON K1N 6N, Canada

[3] Catalysis Centre for Research and Innovation, University of Ottawa, 161 Louis Pasteur, Ottawa, ON K1N 6N, Canada

[4] Department of Sustainable & Renewable Energy, College of Engineering, University of Sharjah, PO Box 27272, Sharjah, UAE

[5] EnPross Incorporated, 147 Banning Road, Ottawa, ON K2L 1C5, Canada

showed that the performance of a direct propane fuel cell was comparable to that obtained with Nafion and aqueous phosphoric acid electrolytes.

Previous evidence in the literature offers an incentive for working at higher temperatures in direct hydrocarbon fuel cells. Higher temperature operation is known to offer an improved tolerance for impurities such as carbon monoxide [4]. However, Nafion and similar PEM's are unlikely to fulfill this target because they lose their proton conductivity due to water loss (dehydration). For example, the proton conductivity of Nafion decreased from 0.066 to 0.00014 S cm^{-1} at 30 °C when the relative humidity (RH) decreased from 100 to 34% [5]. Other studies reported a significant decrease in oxygen reduction rates at RH less than 50% humidity [6]. As a result, many efforts were made in the literature to modify Nafion, or investigate new proton conducting materials.

The incorporation of hygroscopic oxides and solid proton conductors such as Zirconium phosphates (ZrP) in Nafion is one of the approaches proposed in the literature for the synthesis of high temperature membranes. Nafion–ZrP composite membranes were addressed in several studies [7–12]. Following the procedure described by Grot [13], the precipitation of inorganic compounds (such as ZrP) into polymers (such as Nafion) was performed. Membranes were also prepared by the impregnation of Nafion films with a solution of zirconyl chloride and phosphoric acid [14]. Jiang et al. reported Nafion–Teflon–$Zr(HPO_4)_2$ composite membranes [15]. ZrP was also incorporated in polymers such as sulfonated polyetheretherketone (SPEEK) and polybenzimidazole (PBI) [16].

Heteropolyacids (HPAs) represent a type of solid inorganic proton conductors that was addressed in the literature by several studies [17–20]. HPAs such as phosphotungstic acid (PWA) and silicontungstic acid (STA) were added to Nafion [18]. Giordano et al. [21] reported an H_2/O_2 fuel cell with high performance that contained a liquid PWA electrolyte at room temperature. Staiti et al. [22] investigated PWA as a solid composite electrolyte in H_2/O_2. The results showed a poor performance due to the dissolution and loss of PWA. Shao et al. [23] synthesized a hybrid membrane composed of Nafion–silicon oxide doped with PWA for high temperature fuel cells. The conductivity obtained was reported to be much higher than that of Nafion at low RH. Pandey et al. [24] synthesized an ion exchange membrane by impregnating a porous poly vinyldene fluoride (PVDA) film with silica and PWA particles. Composite membranes based on Phosphotungstic acid (PWA) and silica were studied and reported to have a conductivity of 0.001–0.11 S cm^{-1} [23, 25].

The synthesis of nano composite, Nafion free membranes based on ZrP/PTFE/GLY for high temperature direct hydrocarbon fuel cells was reported in earlier studies [26, 27]. It is the objective of the current work to report the effect of adding Phosphotungstic acid (PWA) and/or silicic acid ($SiO_2 \cdot H_2O$) to zirconium phosphates ZrP/PTFE/Glycerol (GLY) composite membranes. It is also aimed at studying the morphology and proton conductivity of the (PWA–ZrP/PTFE/GLY and Si–PWA–ZrP/PTFE/GLY) composite membranes. To the best of our knowledge, this study has not yet been reported in the literature. Phosphoric acid solutions containing small amounts of PWA or (silicic acid + PWA) were used to react with zirconium oxychloride ($ZrOCl_2 \cdot 8H_2O$) to form modified ZrP within the pores of PTFE.

2 Experimental

2.1 Synthesis of PWA–ZrP/PTFE/GLY and Si–PWA–ZrP/PTFE/GLY composite membranes

Porous Unlaminated Sterlitech polytetrafluoroethylene (PTFE) films (pore size = 0.22 μm) were used as the composite membrane support material. The proton conducting material (Zirconium phosphates (ZrP)) was precipitated within the pores of the polytetrafluoroethylene (PTFE) films according to the chemical reaction described in Eq. (1) [28]:

$$ZrOCl_2 \cdot 8H_2O + 2H_3PO_4 \rightarrow Zr(HPO_4)_2 \cdot H_2O + 2HCl + 8H_2O \quad (1)$$

In order to perform the in situ reaction, $ZrOCl_2 \cdot 8H_2O$ was introduced first into the pores of PTFE. This was done by preparing an alcoholic suspension contains zirconium oxychloride, $ZrOCl_2 \cdot 8H_2O$ (purchased from Sigma Aldrich), iso-propyl alcohol (EMD Millipore, HPLC grade, assay 99.8%), and a specific amount of glycerol. The alcoholic suspension was heated, stirred and continuously dripped on top of a rotating PTFE porous film. The alcohol suspension appeared to wet the PTFE film completely. Dripping was stopped on a periodic basis to allow the alcohol to evaporate as the membrane rotates. The alcohol evaporation left the $ZrOCl_2 \cdot 8H_2O$ behind. Phosphotungstic acid (PWA)-ZrP/PTFE/GLY and PWA–Silicic acid–ZrP/PTFE/GLY membranes were prepared by adding specific amounts of phosphotungstic acid (PWA), $H_3[P(W_3O_{10})_4] \times H_2O$ (Sigma Aldrich reagent grade), silicic acid, $SiO_2 \cdot H_2O$ (+80 mesh powder, from Sigma Aldrich) or both, to phosphoric acid, H_3PO_4. Phosphotungstic acid (PWA), Glycerol (GLY) and silicic acid were added to phosphoric acid at a mass ratio of 0.2 with respect to the produced ZrP. To achieve this modification, the membranes were then immersed in 20 mL H_3PO_4 (contained phosphotungstic acid (PWA), silicic acid (SiO_2. H_2O) or

both of them); for 72 h to perform the reaction described in Eq. (1). The membranes were gently rinsed after that with deionized water to remove the formed HCl and dried in the oven for 24 h at 120 °C. Two types of modified ZrP/PTFE/GLY membranes were synthesized in this work. The first one was modified by phosphotungstic acid (PWA) that was added to H_3PO_4. The second was modified by both, PWA and silicic acid $SiO_2{\cdot}H_2O$, added to H_3PO_4.

2.2 Characterization of the synthesized membranes

2.2.1 *Investigation of the composite membrane proton Conductivity*

The modified membranes were investigated for their proton conductivity using electro-chemical impedance spectroscopy (EIS). EIS measurements were performed at room temperature by the four probe method. A schematic diagram showing the cell connections in the four probe method is presented in Fig. 1.

The EIS measurements were performed using a Parstat 2273 instrument and Power Suite 2.58, 2003 electrochemical software. The frequency range was of 1–100 kHz. The membrane sample was placed in between stainless steel electrodes. Nyquist plots were obtained, from which, the resistance R (Ohms) was determined from the intercept with the real impedance axis. The cell diameter is 7.08 mm, of which the cross sectional area is calculated. The membrane thickness, d in cm, was measured. The proton conductivity σ in Siemens per centimeter (S cm^{-1}), was then calculated using Eq (2) [26].

$$\sigma = d/(R \times A) \quad (2)$$

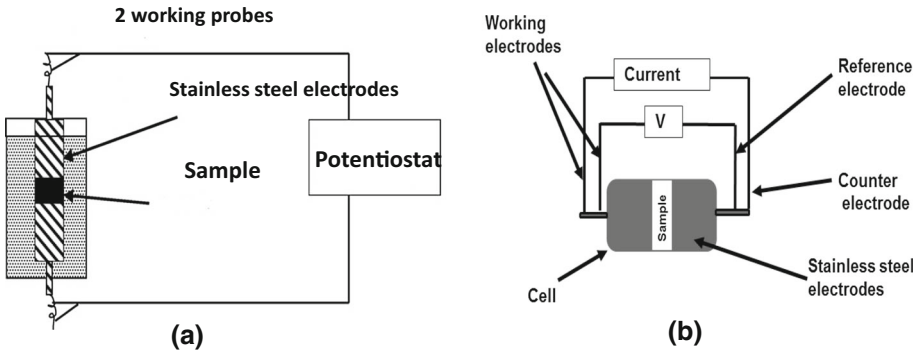

Fig. 1 A schematic diagram shows the cell connections (**a**) and the four probe method (**b**)

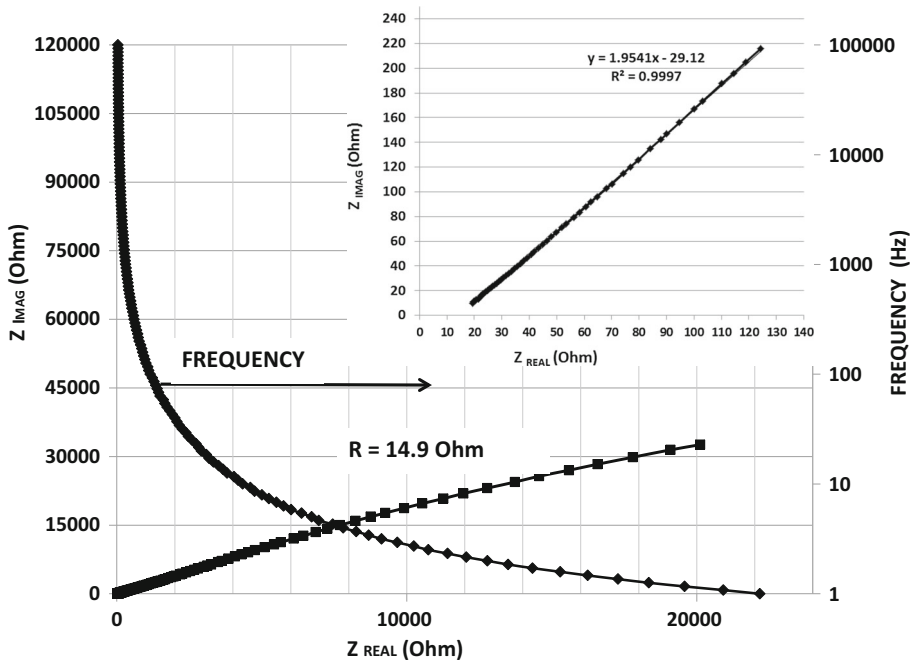

Fig. 2 Nyquist plot for the composite membrane modified with Phosphotungstic acid (PWA). The PWA/ZrP and GLY/ZrP mass ratios = 0.2

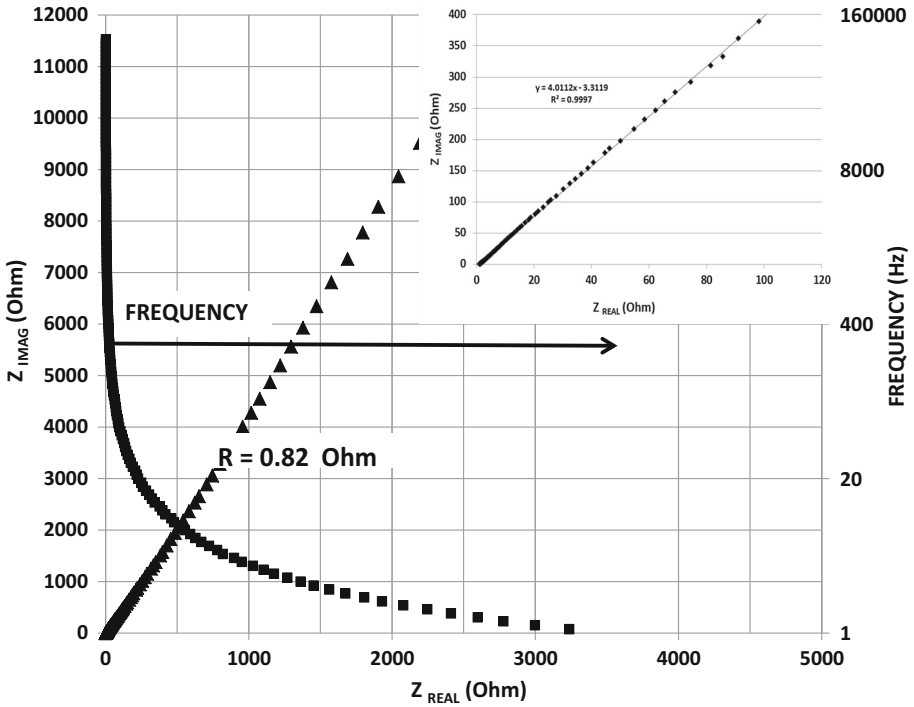

Fig. 3 Nyquist plot for the samples of the composite membrane modified with Phosphotungstic acid (PWA) and silicic acid (PWA–Si–ZrP/PTFE/GLY membrane). The PWA/ZrP and GLY/ZrP mass ratios = 0.2

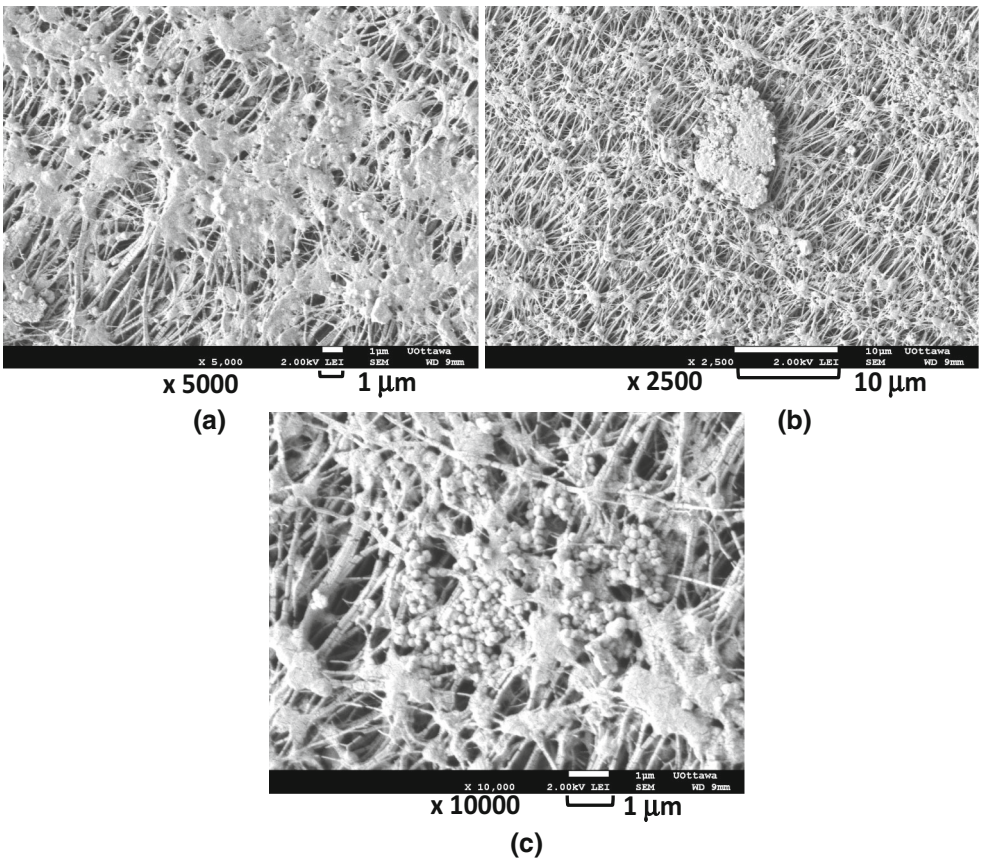

Fig. 4 SEM images for a PWA–ZrP/PTFE/GLY composite membrane, at a GLY/ZrP mass ratio of 0.2. at different magnifications (**a–c**)

2.2.2 Characterization of the synthesized samples using scanning electron microscopy (SEM) and energy-dispersive X-ray spectroscopy (EDS)

SEM and EDS were performed on the synthesized membrane samples using a JEOL JSM-7500F Field Emission Scanning Microscope at various magnifications.

3 Results

3.1 Proton conductivity

EIS measurements were performed to study the proton conductivity of the synthesized PWA–ZrP/PTFE/GLY composite membranes. Figure 2 shows the Nyquist plot obtained along with the frequency range from EIS. The results reported here with modified ZrP having a PWA component will be compared to previously reported results with modified ZrP that did not contain a PWA component [27]. The composite membrane resistance, R (Ohm) was obtained from the intercept of the Nyquist plot with the x-axis. The resistance (14.9 Ohms) along with the thickness of the sample were used in Eq. (2) to calculate the proton conductivity, σ (S cm^{-1}). A proton conductivity of 0.003 S cm^{-1} was obtained for the PWA–ZrP/PTFE/GLY membrane. The measured proton conductivity for the ZrP/PTFE/GLY membrane that did not have a PWA component was 0.045 S cm^{-1} [27]. In this case, the presence of PWA decreased the conductivity by a factor of 15 for ZrP membranes that did not include a PWA component.

EIS measurements were also performed on the membrane modified by Phosphotungstic acid (PWA) and Silicic acid, i.e., (PWA–Si–ZrP/PTFE/GLY) composite membrane. The results are shown in Fig. 3. The resistance obtained from the Nyquist plot = 0.82 Ohms. It was noticed that there is a decrease in the resistance of the composite membrane. The proton conductivity, σ (S cm^{-1}) was calculated using Eq. (2). A proton conductivity of 0.059 S cm^{-1} was calculated for the PWA–Si–ZrP/PTFE/GLY membrane. In comparison with the conductivity calculated from the data in Fig. 2 (0.003 S cm^{-1}), it was noticed that the addition of PWA and silicic acid increased the proton conductivity by a factor of 20.

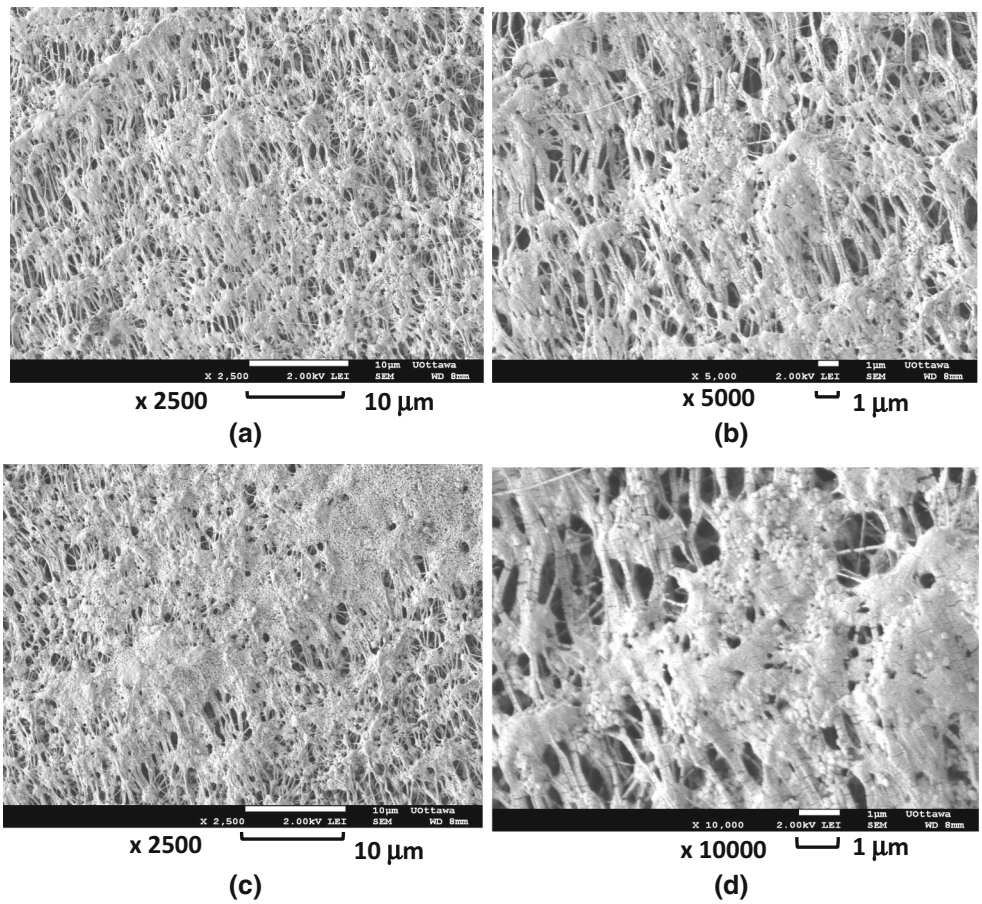

Fig. 5 SEM images for a Si–PWA–ZrP/PTFE/GLY composite membrane, at a GLY/ZrP mass ratio of 0.2. and Silicic acid/ZrP mass ratio of 0.2. at different magnifications

3.2 Morphology studies

Scanning electron microscopy (SEM) imaging was performed on the ZrP modified membranes containing the PWA component. The results are shown in Fig. 4a–c.

Previously, the ZrP/PTFE/GLY composite membranes revealed the formation of nearly spherical ZrP particles, in the size range of 250–500 nm [28]. SEM images shown in Fig. 4a–c show the presence of a plate-like material that does not completely cover the PTFE pores. Empty PTFE pores can be seen in the synthesized composite membrane. In addition, SEM imaging showed a few particles that appeared to have some cubic structure (Fig. 4a, b).

In this work, it is apparent that the addition of PWA caused a change in the material morphology. It is evident from Fig. 4a–c that a flaky agglomerate was formed of about 10 microns in size (Fig. 4b). Also, very small nearly spherical particles of 150 nm in size were observed in other regions. These nano-size particles appear to be suspended around the PTFE nodes (Fig. 4c). This change in morphology, compared to ZrP/PTFE/GLY, was accompanied by a change in proton conductivity. The reported proton conductivity for the ZrP/PTFE/GLY membranes that did not contain a PWA component was 0.045 S cm^{-1} [27, 28]. The calculated proton conductivity for the PWA modified membranes shown in Fig. 4 was 0.003 S cm^{-1}.

Proton conductivity is known to occur by Grothuss or hopping mechanism [29]. Protons hop between the oxygen atoms in the OH groups of molecules such as water, glycerol and Zirconium phosphates (ZrP) [30]. Protons can hop in the bulk of liquid or solid. They can also hop on the surface. The proton conductance in ZrP was shown to be a function of morphology [31, 32]. Alberti et al. [31, 32] described the effect of surface protons on conductivity. Although the fraction of surface protons is small, their mobility is 10^4 times greater than the protons in bulk of ZrP. This implies that greater external ZrP surface area, results in greater proton conductivity [32]. Hence, one possible explanation for the decrease in proton conductivity for the PWA-modified membrane can be attributed to the decrease in the total surface area of ZrP particles due to the formation of larger particles.

Heteropolyacids, such as Phosphotungstic acid (PWA), are known to be good proton conductors. Information in the literature describes protons being attached to the oxygen atoms by hydrogen bonds inside their Keggin unit structure [33]. Ganapathy et al. [33] also reported that heteropolyacids possess high proton mobility in their hydrated form.

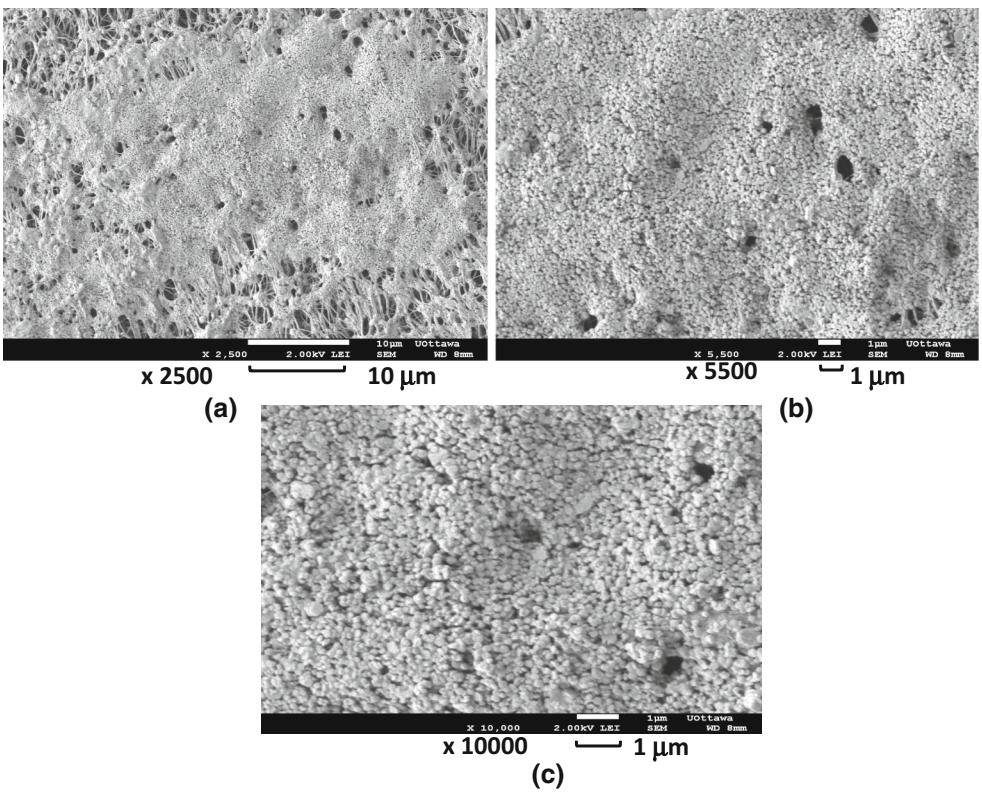

Fig. 6 SEM images for a Si–PWA–ZrP/PTFE/GLY composite membrane, at a GLY/ZrP mass ratio of 0.2. and Silicic acid/ZrP mass ratio of 0.2. at different magnifications

Their conductivity is in the range (0.02–0.1 S cm^{-1}) [34]. Therefore, it was expected that the modification of ZrP with PWA would increase the proton conductivity. However, PWA is also water soluble [22, 23]. The 85% H_3PO_4 used in this work contains water. In addition, the membrane was washed with deionized water. As a result, part of the PWA that was introduced into the membrane might have been dissolved. Based on SEM pictures, less coverage of the material was observed on the PTFE surface. Overall, the modification of the synthesized membrane using PWA was expected to increase the proton conductivity. In contrast, the proton conductivity decreased when PWA was added to the ZrP/PTFE/GLY membrane.

Table 1 A Summary of conductivity results in S cm^{-1} for the modified composite membranes. PWA/ZrP and GLY/ZrP mass ratios = 0.2, Si/P mass ratio = 0.4

Type of membrane	Conductivity (σ) [S cm^{-1}]	Reference
ZrP/PTFE/GLY	0.045	[27]
PWA–ZrP/PTFE/GLY	0.003	This work
PWA–Si–ZrP/PTFE/GLY	0.059	This work
Nafion–silica–PWA	0.023	[23, 35]
Si–ZrP/PTFE/GLY	0.056	[28]
ZrP powder	7.04×10^{-5}	[26]

Figure 5 shows a top view SEM images for of the ZrP membrane that contained PWA and silicic acid (PWA–Si–ZrP/PTFE/GLY) at different magnifications. In general, the formation of a flaky material and the presence of an open structure as observed in images (a) through (d). At higher magnifications, as can been in images (b and d), small particles in the size of 150 nm were observed to be embedded in the flaky shape material. Figure 6 shows another type of morphology observed in the Si–PWA–ZrP/PTFE/GLY membranes. Nearly spherical particles of 150 nm in size appear to uniformly cover the top of the membrane with some pores still shown (Fig. 6c).

Examination of the SEM images shows that there was a variation in morphology of the material in the PWA modified membrane. A proton conductivity of 0.059 S cm^{-1} was calculated for the PWA–Si–ZrP/PTFE/GLY membrane. This conductivity is higher than that for Nafion/SiO_2/PWA membrane reported in the literature by Shao et al. [35]. It is also about 20 times higher than that obtained for the PWA–ZrP/PTFE/GLY membrane in this study. This enhancement in proton conductivity upon the introduction of silicic acid along with PWA can be attributed to the following reasons:

1. As seen in SEM, the formation of smaller, nano-size ZrP spherical particles within the pores of PTFE that

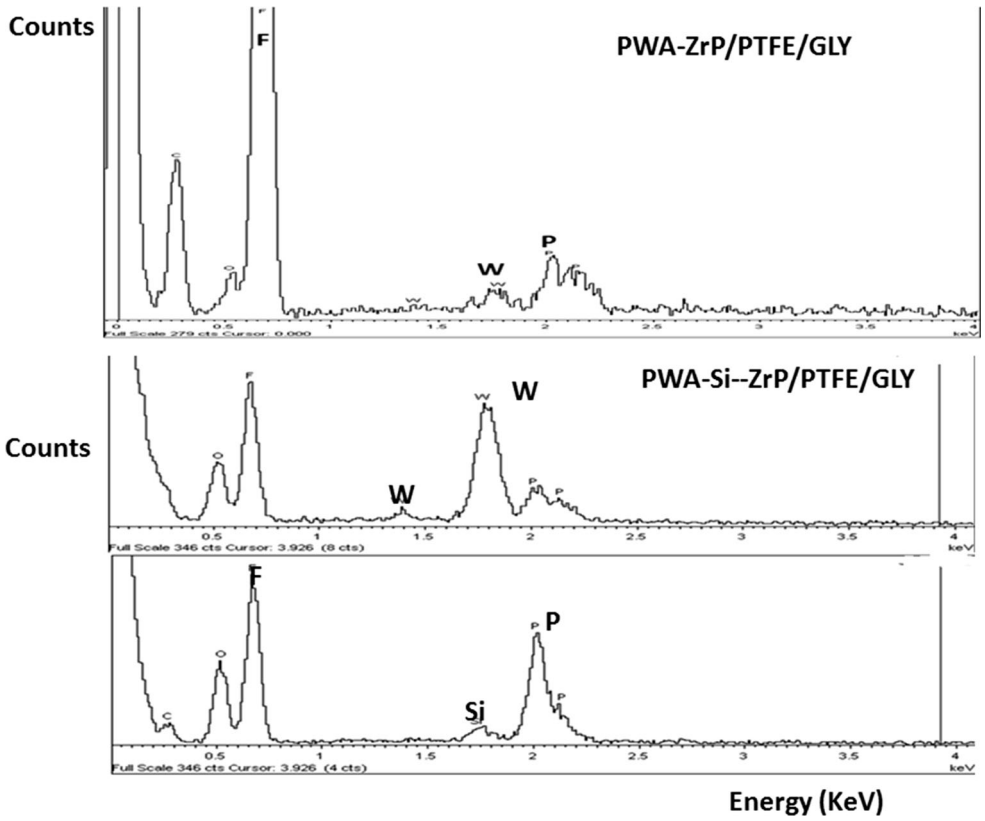

Fig. 7 EDS analysis performed on the PWA–ZrP/PTFE/GLY and PWA–Si–ZrP/PTFE/GLY composite membranes

resulted in the increase in the total surface area, hence, an increase in the proton conductivity.

2. The presence of silicic acid might have improved water uptake due to its hydrophilic nature [28]. In addition, some silicic acid appeared to be dissolved in H_3PO_4, thus, it is expected that some Si atoms replaced some of the P atoms in the ZrP lattice as shown in an earlier work [28] leading to an increase in proton conducting paths.
3. Although PWA is water soluble, but it is well known that it can be immobilized by the addition of silica gel [36, 37]. In addition, it was shown in the literature that PWA interacts with silica [38]. The membrane that contained PWA and silicic acid appeared to have smaller size ZrP particles hence, enhanced proton conductivity.

A summary of proton conductivity results are shown in Table 1. It can be clearly seen that adding PWA alone decreased the conductivity of the ZrP/PTFE/GLY membranes by a factor of 15. However, when PWA addition was combined with silicic acid, the membrane's conductivity increased from 0.003 to 0.059 S cm^{-1}. This conductivity reported in this work for the PWA–Si–ZrP/PTFE/GLY membrane is higher than that reported for Nafion–Silica–PWA membrane.

Figure 7, shows the EDS analysis performed on the PWA–Si–ZrP/PTFE/GLY composite membranes. The analysis confirmed the presence of a fluorine "F" peak, tungsten "W", silicon "Si" and phosphorus "P" peaks. EDS analysis performed on PWA–ZrP/PTFE/GLY composite membrane confirmed the presence of the "W", "P" and a larger "F" peak. Such larger and more intense "F" peak is consistent with the less coverage of the PTFE surface as seen in SEM pictures.

4 Conclusions

Phosphotungstic acid (PWA) was found to have a negative effect resulting in the decrease in the PWA–ZrP/PTFE/GLY proton conductivity by a factor of 15 compared to the unmodified ZrP/PTFE/GLY composite membrane. The addition of PWA + silicic acid led to an increase in proton conductivity compared to that observed in the PWA–ZrP/PTFE/GLY membrane. The proton conductivity increased by a factor of 20 in the PWA–Si–ZrP/PTFE/GLY membrane as opposed to PWA alone–ZrP/PTFE/GLY membrane. This enhancement in proton conductivity for the PWA–Si–ZrP/PTFE/GLY membrane is consistent with the formation of smaller, nano sized ZrP particles that increased the total surface area, hence, proton conductivity. The presence of PWA alone appeared to negate the positive effect of GLY on proton conductivity that was previously reported [27]. The porous structure observed for the PWA–Si–ZrP membranes along with the reasonable reported proton conductivity in this work (i.e., 0.059 S cm^{-1}) is higher the proton conductivity of Nafion–Si–PWA membranes and would make them suitable as the electrolyte component in the catalyst layer for fuel cell applications.

Acknowledgements The authors are grateful for the financial support from the American University of Sharjah provided through the faculty research travel grant, FRG15-T-21 and FRG14-3-13.

References

1. O. Savadogo, F.J.R. Varela, J. New Mater. Electrochem. Syst. **4**, 93–97 (2001)
2. H. Khakdaman, Y. Bourgault, M. Ternan, Ind. Eng. Chem. Res. **49**, 1079–1085 (2010)
3. H. Khakdaman, Y. Bourgault, M. Ternan, J. Power Sour. **196**, 3186–3194 (2011)
4. C. Yang, P. Costamagna, S. Srinivasan, J. Benzider, A.B. Bocarsly, J. Power Sour. **103**, 1–9 (2001)
5. J.L. Zhang, Z. Xie, J. Zhang, Y. Tang, C. Song, T. Navessin, Z. Shi, D. Song, H. Wang, D. Wilkinson, Z. Liu, S. Holdcroft, J. Power Sour. **160**, 872–891 (2006)
6. C. Neyerlin, H.A. Gasteiger, C.K. Mittelsteadt, J. Jorne, W.B. Gu, J. Electrochem. Soc. **152**, A1073–A1108 (2005)
7. F. Bauer, M. Willert-Porada, J. Membr. Sci. **233**, 141–149 (2004)
8. H.C. Kuan, C.S. Wu, C.Y. Chen, Z.Z. Yu, A. Dasari, Y.W. Mai, Electrochem. Solid State Lett. **9**, A76–A79 (2006)
9. E. Chalkova, M.V. Fedkin, S. Komarneni, S.N. Lvov, J. Electrochem. Soc. **154**, B288–B295 (2007)
10. D. Truffier-Boutry, A. De Geyer, L. Guetaz, O. Diat, G. Gebel, Macromolecules **40**, 8259–8264 (2007)
11. C. Yang, S. Srinivasan, A.S. Arico, P. Creti, V. Baglio, V. Antonucci, Electrochem. Solid-State Lett. **4**, A31–A34 (2001)
12. G. Alberti, M. Casciola, A. Donnadio, R. Narducci, M. Pica, M. Sganappa, Desalination **19**, 280–282 (2006)
13. W.G. Grot, G. Rajendran, US Patent 5,919,583, 1999
14. P. Costamagna, C. Yang, A. Bocarsly, S. Srinivasan, Electrochim. Acta **47**, 1023–1033 (2002)
15. R. Jiang, H.R. Kunz, J. Fenton, Electrochim. Acta **51**, 5596–5605 (2006)
16. Q. Li, R. He, J. Jensen, N.J. Bjerrum, Chem. Mater. **15**, 4896–4915 (2003)
17. V. Neburchilov, J. Martin, H. Wang, J. Zhang, J. Power Sour. **169**, 221–238 (2007)
18. B. Tazi, O. Savadogo, J. New Mater. Electrochem. Syst. **4**, 187–196 (2001)
19. B. Tazi, O. Savadogo, Electrochim. Acta **45**, 4329–4339 (2000)
20. M. Helen, B. Viswanathan, S. Srinivasa, Murthy. J. Membr. Sci. **292**, 98–105 (2007)
21. N. Giordano, P. Staiti, S. Hocevar, A.S. Aricò, Electrochim. Acta **41**, 397–403 (1996)
22. P. Staiti, S. Hocevar, N. Giordano, Int. J. Hydrogen Energy **22**, 809–814 (1997)
23. Z.G. Shao, P. Joghee, I.-M. Hsing, J. Membr. Sci. **229**, 43–51 (2004)
24. J. Pandey, A. Shukla, Mater. Lett. **100**, 292–295 (2013)
25. Y. Zhou, J. Yang, H. Su, J. Zeng, S.P. Jiang, W.A. Goddard, J. Am. Chem. Soc. **136**, 4954–4964 (2014)

26. A. Al-Othman, A.Y. Tremblay, W. Pell, S. Letaief, T.J. Burchellc, B.A. Peppley, M. Ternan, J. Power Sour. **195**, 2520–2525 (2010)
27. A. Al-Othman, A.Y. Tremblay, W. Pell, Y. Liu, B.A. Peppley, M. Ternan, J. Power Sour. **199**, 14–21 (2012)
28. A. Al-Othman, A.Y. Tremblay, W. Pell, S. Letaief, Y. Liu, B.A. Peppley, M. Ternan, J. Power Sour. **224**, 158–167 (2013)
29. K.-D. Kreuer, Chem. Mater. **8**, 610–641 (1996)
30. M. Nogami, R. Nagao, C. Wong, T. Kasuga, T. Hayakawa, J. Phys. Chem. B **103**, 9468–9472 (1999)
31. G. Alberti, E. Torracca, J. lnorg. Nucl. Chem. **30**, 1093–1099 (1968)
32. G. Alberti, M. Casciola, U. Costantino, G. Levi, G. Ricciardi, J. Inorg. Nucl. Chem. **40**, 533–537 (1978)
33. S. Ganapathy, M. Fournier, J.F. Paul, L. Delevoye, M. Guelton, J.P. Amoureux, J. Am. Chem. Soc. **124**, 7821–7828 (2002)
34. U. Mioc, M. Davidovic, N. Tjapkin, P. Colomban, A. Novak, Solid State Ion. **46**, 103–109 (1991)
35. Z.G. Shao, H. Xu, M. Li, I.-M. Hsing, Solid State Ion. **177**, 779–785 (2006)
36. S.M.J. Zaidi, S.D. Mikhailenko, G.P. Robertson, M.D. Guiver, S. Kaliaguine, J. Membr. Sci. **173**, 17–34 (2000)
37. L.T. Aany Sofia, A. Krishnan, M. Sankar, N.K. Kala Raj, P. Manikandan, P.R. Rajamohanan, T.G. Ajithkumar, J. Phys. Chem. C **113**, 21114–21122 (2009)
38. P. Staiti, S. Freni, S. Hocevar, J. Power Sour. **79**, 250–255 (1999)